



Separation of protein SH-variants

Beate Hintersteiner

6 months research stay at the Lawrence Berkeley National
Laboratory

03-02-2015 – 08-28-2015



1. Introduction

1.1. Microheterogeneity of monoclonal antibodies and SH-variants

Over the last decade biological therapeutic products have become an increasingly important class of pharmaceuticals and the market for these drugs is still growing rapidly. In 2012 biologicals showed a sales increase of 18.2 % in the US compared to 2.5% for the pharmaceutical sector overall. The top-selling products among this new class of therapeutics are monoclonal antibodies (mAbs), which made up for nearly 40% of biologicals sold in the US in 2012 [1]

Being comparatively large and structurally complex biomolecules, monoclonal antibodies contain many target points for modifications, which include different post-translational processing reactions, done in the cell as well as chemical modifications that happen mostly during storage. The most common modifications result from different glycosylation patterns, N-terminal glutamine cyclization, C-terminal lysine processing, deamidation of asparagine and glutamine, oxidation of methionine, glycation, incomplete signal peptide cleavage as well as the formation of alternative thiol structures. (Figure 1)

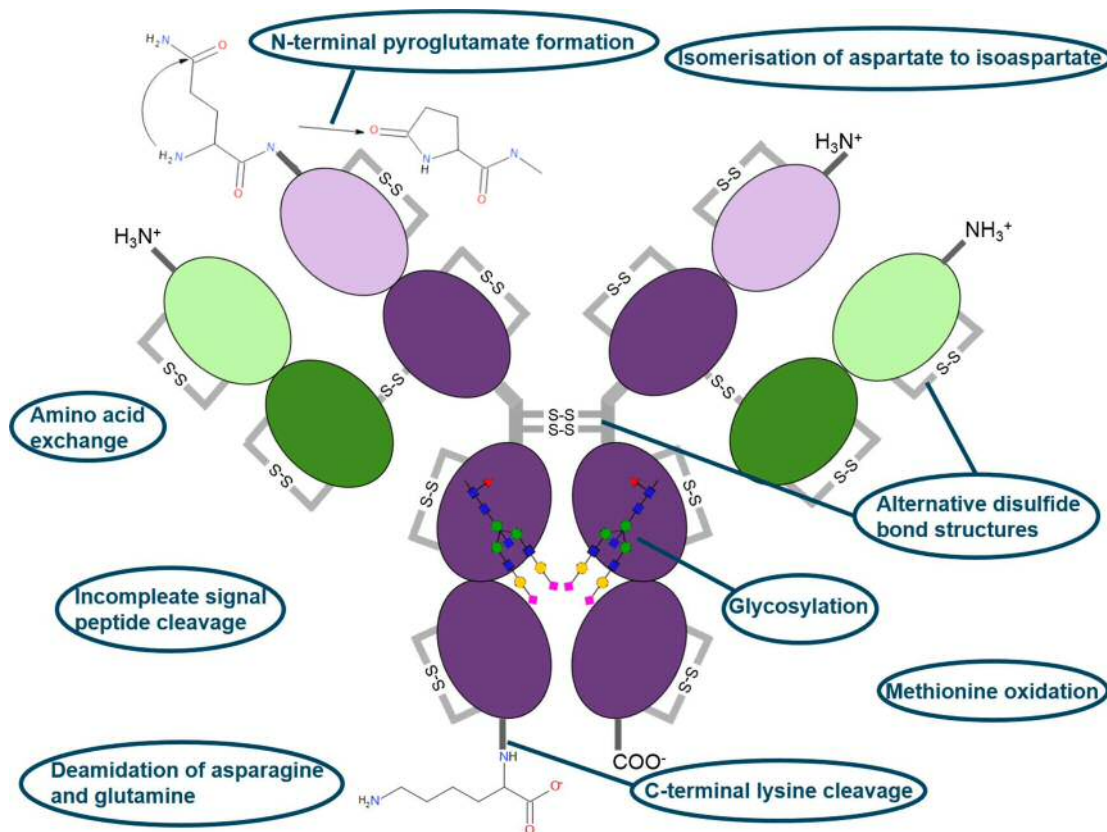


Figure 1 Structure and possible modifications of a monoclonal antibody

The biotechnological production of monoclonal antibodies does therefore not lead to only one defined species of molecules, but rather to a large variety of so-called isoforms, which may differ in structure, biophysical characteristics (e.g. the pI values), stability as well as biological activity.

[2] This phenomenon is described as microheterogeneity and it is considered to be a critical quality attribute for monoclonal antibodies [3], which means that it has to be monitored during production as far as possible.

In order to be able to closely monitor and further investigate the microheterogeneity of monoclonal antibodies, however, there is a need for high resolution analytical methods that would allow the separation and characterization of different protein variants. Recently, successful attempts at developing a better chromatographic method for the separation of antibody charge variants have been reported. [4, 5] The term charge variants describes all sorts of isoforms present in a protein samples, which differ in their charge state or, speaking in less abstract terms, contain different numbers of positively or negatively charged building blocks.

However, only a small proportion of all the modifications possible in a given protein result in an altered charge state. There are many other types of possible protein variants that cannot be separated by charge based methods alone. One of those are the so-called thiol or SH-variants. The term thiols describes all the sulfhydryl-groups (SH-groups) present in a molecule. With respect to proteins any SH-groups present are resulting from the amino acid cysteine. (Figure 2) Thiol groups are of highly reactive chemical nature and can participate in various kinds of interactions with other molecules, including the binding to noble metals like gold or silver. The biologically most important reaction of SH-groups, however, is the formation of disulfide bonds (S-S bonds).

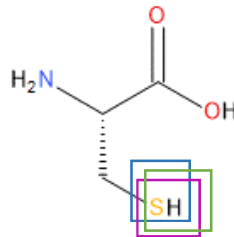


Figure 2 Cysteine and its thiol group

As disulfide bonds are the only covalent and therefore most stable crosslinks commonly found in polypeptide chains the correct formation of these bonds is of profound importance for assembly and maintenance of the active folding state of a protein.

As a result the formation of different thiol structures ranging from trisulfide bonds and non-reducible thioether linkages to free SH-groups in proteins in general and monoclonal antibodies in particular, pose a highly relevant and very interesting research target. An entirely chromatographic method for the separation and analysis of thiol variants of different proteins would enormously facilitate the investigation of this class of protein variants.

1.2. Monolithic chromatography columns and nanoparticles for separation sciences

Monoliths as stationary phases for chromatographic processes were introduced in the early 1990s. In contrast to traditional chromatography columns made from packed beds of particles, monolithic columns consist of a single block of separation media containing large and interconnected through pores. The driving force of mass transfer in these monoliths is convective flow rather than diffusion. This allows the use of much higher flow rates in separation processes

without encountering the issues of high back pressure and low efficiencies due to diffusional mass transport limitations associated with classical particulate separation media. [6-9]

Monolithic columns are either made from silica or from organic polymers. Polymer based monoliths are normally prepared by copolymerization of a functional monomer and a crosslinker substance in the presence of organic solvents, serving as porogens. [10-12] This approach, however, leads to a certain number of problems. Those include the lack of availability of monomers with functional groups suitable for certain types of chromatography, the risk that a significant number of functionalities may not be available for use in separation processes because they lie protected inside the dense polymer structure, as well as the time-consuming need to optimize the reaction conditions for every new monomer used. [13]

The easiest way to overcome those limitations is the chemical modification of the surface of previously prepared monoliths, which allows the introduction of numerous different functionalities onto the same kind of parent monoliths. One possibility of how to introduce certain desired chemical properties onto the surface of a monolith, is the attachment of nanoparticles. [14-16]

Silver nanoparticles in the size range below 100nm are an interesting option for the separation sciences because of their high surface area-to-volume ratio and their size compatibility with large biomolecules like proteins. [17] Furthermore they are readily available and can relatively easily be prepared in the laboratory. [18]

There have been previous attempts at the Berkeley lab to use monolithic columns covered with gold nanoparticles as a stationary phase for a chromatographic separation method for protein SH-variants. However, the interaction between the gold nanoparticles and the SH-groups containing proteins proved to be too strong to achieve elution of the proteins once they were bound to the nanoparticle columns.

The affinity of thiols towards silver, however, is known to be lower than towards gold. As a result silver nanoparticles might prove to be a superior basis for developing a separation method for thiol variants in proteins.

2. Materials and Methods

2.1. Materials

Glycidyl methacrylate (GMA), ethylene dimethacrylate (EDMA), cyclohexanol, 1-dodecanol, azobisisobutyronitrile (AIBN), 3-(trimethoxysilyl)propyl methacrylate, 2-mercaptoethanol, aluminum oxide (basic alumina), cystamine dihydrochloride, tris(2-carboxyethyl)phosphine hydrochloride (TCEP), HPLC-grade acetonitrile, silver nitrate, sodium citrate dihydrate, sodium borohydrate, methanol, hydrochloric acid, albumin from human serum, myoglobin, cytochrome C from *S. cerevisiae*, bovine serum albumin BSA, acetone, 2-mercaptopropionic acid and Sodium 2-mercaptoethanesulfonate were all purchased from Sigma-Aldrich (St. Louis, MO, USA). Water delivered by an EASYpure® II LF ultrapure water purification system (Barnstead, Boston, MA, USA) was used for all experiments. Polyimide coated fused silica capillaries (100 µm I.D.) were purchased from Polymicro Technologies (Phoenix, AZ, USA).

2.2. Instrumentation

A syringe pump (Kd Scientific, New Hope, PA, USA) was used for the modification of monolithic columns with cystamine and TCEP. The silver nanoparticle dispersion was pumped through the monolithic columns using a high pressure 100DM syringe pump (Teldyne ISCO, Lincoln, NE, USA). All HPLC experiments were carried out using a Waters Acquity UPLC system.

As an HPLC-MS system, a Bruker Daltonics MicroTOFQ ESI-instrument connected to an Agilent 1200 Infinity HPLC was used.

2.3. Synthesis of silver nanoparticles

50mL each of a 2.5mM aqueous AgNO₃ solution and a 3.1mM aqueous sodium citrate dihydrate solution were prepared and cooled to 4°C.

A round flask and a magnetic stirrer were washed with Methanol, 5M HCl, and then multiple times with H₂O to remove the solvent and the acid. The AgNO₃ and the sodium citrate solution were mixed in this flask while stirring and 3mL of 2.5mM aqueous NaBH₄ solution were added rapidly to allow the initial seeding of the nanoparticles. The flask was closed with two septa, a needle was inserted for ventilation and the mixture was left to stir for 10min. Then the flask was put into an oil bath, which was heated to 80°C, and left stirring at this temperature for another 90min. Afterwards the reaction was quenched by putting it into an ice bath.

The color of the solution changed from colorless to a reddish brown when adding NaBH₄ and then became more and more yellow while stirring at higher temperature.

The nanoparticle solution obtained from this synthesis was then aliquoted into 20mL glass vials and stored at 4°C.

The quality of the nanoparticles was checked by Transmission electron microscopy (TEM), the size distribution of the particles was calculated based on those TEM-pictures using the Image J Software.

2.4. Surface modification of the capillary wall

Approx. 3m of a 100µM capillary were cut and first rinsed with 2mL acetone, followed by 2mL water using using a syringe pump. Then 2 solutions of 0.2M NaOH and 0.2M HCl were prepared and then used to flush the capillary. First NaOH was pumped through the column until a basic pH could be detected and then for an additional 30min at a flow rate of 0.25µL/min (=0.015mL/h). Afterwards the capillary was rinsed in the same way with 0.2mol HCl. In between as well as after the HCl step water was pumped through the capillary until neutral pH could be detected at the open end. Afterwards the capillary was rinsed with ethanol and the derivatization reagent was prepared. Therefore 200µL of 3-(trimethoxysilyl)propyl methacrylate was mixed with 800 µl of ethanol (previously adjusted to pH 5 with acetic acid) and the mix was then pumped through the capillary at a flow rate of 0.25 µL/min for 60min. Finally the capillary was rinsed with acetone and blow-dried with pressurized nitrogen. The ends were sealed with rubber caps and the column was left in this stage for 24 hours at room temperature to allow the condensation reaction of the silanol groups to complete. Afterwards the capillary was cut into pieces of different length.

2.5. Polymerization of the monolith

Both monomers Glycidyl methacrylate (GMA) and ethylene dimethacrylate (EDMA) were purified by passing them through an aluminum column to remove inhibitors and then filtered through a 0.2 μ m syringe filter to avoid aluminum contaminations in subsequent steps. Then a polymerization mixture containing 24 % GMA, 16% EDMA, 30% cyclohexanol, 30% 1-dodecanol and 1% AIBN initiator with respect to total monomer content was prepared, sonicated for 15min and purged with liquid nitrogen for 10min.

The vinylized capillaries described above were then filled with this mixture, sealed with rubber caps at both ends and kept at a 60°C water bath for 24h.

Afterwards the porogens cyclohexanol and 1-dodecanol were removed by pumping acetonitrile through the column for 30min at a flow rate of 3 μ L/min.

2.6. Backpressure test

In order to control the quality of the monolithic capillary columns prepared above the column backpressure was checked when pumping Acetonitrile through the column at a flow rate of 1 μ L/min. This experiment should result in a column backpressure value between 5 and 8bar/cm column length.

2.7. Reaction with cystamine, ethanolamine and tris(2-carboxyethyl)phosphine

A 1M cystamine dihydrochloride solution was prepared in 2mol/L aqueous sodium hydroxide and pumped through the monoliths at a flow rate of 0.5 μ L/min for 1h at room temperature. The capillaries were then sealed with rubber caps and put into a 50°C water bath for 1h. These two steps were then repeated once again and afterwards the columns were washed with water until neutral pH could be detected in the eluent.

Unreacted epoxy groups were then capped with ethanolamine by pumping a 1mol/L solution (pH 8.5) through the columns at a flow rate of 0.5 μ L/min for one hour. Afterwards the column was again flushed with water until the pH of the eluent was neutral.

In order to cleave the disulfide bonds of the immobilized cystamine and obtain free SH-groups on the monolith a 0.25mol/L tris(2-carboxyethyl)phosphine (TCEP) solution was then pumped through the column at a flow rate of 0.25 μ L/min for 2hours. The columns were then once again washed with water until a neutral pH could be detected in the eluat.

2.8. Modification with silver nanoparticles

A 3mL loop was filled with the previously prepared silver nanoparticle dispersion, which was then pumped through the functionalized monoliths at a flow rate of 1 μ L/min until the eluent turned yellow. Afterwards the columns were rinsed with water for 30 min at a flow rate of 5 μ L/min and acetonitrile for another 30min at a flow rate of 3 μ L/min.

2.9. Quenching reaction with N-ethylmaleimide

Unreacted thiol groups were quenched by pumping a solution of 0.5M N-ethylmaleimide through the capillary at a flow rate of 0.5 μ L/min for 2h.

2.10. Dead volume testing

Acetone was injected into the HPLC with a nanoparticles modified column connected to the system. Water was used as a mobile phase. Peaks were detected at a wavelength of 214nm.

2.11. Injection of model proteins on silver modified monolith

200nL of a model protein solution at a concentration of 1.5mg/mL were injected at a flow rate of 1 μ L/min. Water was used as mobile phase A. For elution a gradient of mobile phase B, consisting either of 5 M aqueous 3-mercaptopropionic acid, 100mM Sodium 2-mercaptoethanesulfonate (MESNA) or 100% Acetonitrile was run. Peaks were detected at 280nm and 350.

2.12. Regeneration of the nanoparticle column

Elevated temperatures should weaken the interaction between the silver nanoparticles and the thiol groups from the reagent used for elution.

Therefore regeneration was attempted by flushing the columns with water at a flow rate of 1 μ L/min for 2 hours at 2 different temperatures, 65°C and 80°C.

The column oven of the Waters Aquity system was used for heating the column to 65°C, while flushing it with water using the UPLC pump. 65°C, however, is the maximum temperature that can be reached with the system.

So for the 80°C procedure a different set up, had to be used. This time, the column was connected to the high pressure syringe pump via a long inlet line, submerged in an 80°C waterbath and connected to an outlet line in order to avoid contaminating the water bath with eluent from the column.

2.13. Injection of nanoparticles and nanoparticle/protein mixture

A 1:100 dilution of silver nanoparticles in water was injected into the HPLC without any column connected to the system. Afterwards a mixture of nanoparticles (1:100 dilution in water) and human serum albumin (1.5mg/mL) was injected. In both experiments water was used as the mobile phase and signals were detected for 15min at 2 different wavelengths, 280 and 350nm, the flow rate was 1 μ L/min.

3. Results and Discussion

3.1. Attachment of silver nanoparticles to a monolithic column

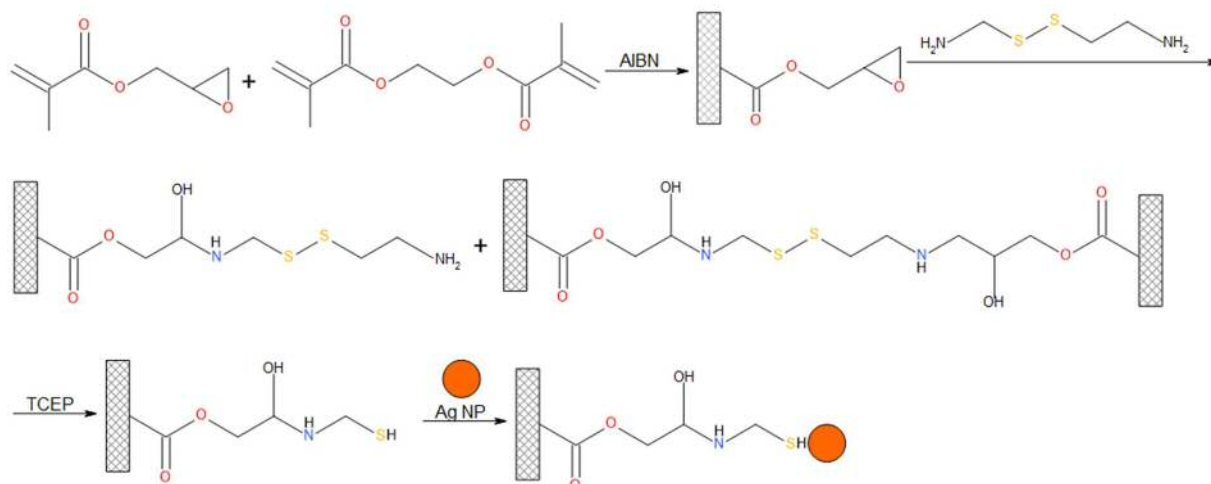


Figure 3 Reaction scheme for the surface modification of a monolithic column with silver nanoparticles

Figure 3 shows the different modification steps necessary for the surface modification of a monolithic column with silver nanoparticles. First of all the two monomers Glycidyl methacrylate (GMA) and ethylene dimethacrylate (EDMA) are polymerized by adding the crosslinker azobisisobutyronitrile (AIBN) to form the initial monolith, resulting in a surface rich with epoxy groups. Addition of cystamine introduces a large number of disulfide bridges, which can then be cleaved by tris(2-carboxyethyl)phosphine (TCEP), providing free SH-groups on the surface of the monoliths. Those SH-groups allow the assembly of a layer of silver nanoparticles due to the high affinity of those particles towards thiol groups.

3.2. Model proteins

Due to their highly reactive nature, any free thiol groups in a protein, represent potential target sites for various kinds of chemical reactions. Examples include simple oxidation reactions as well as more complex ones, like the formation of intra-molecular disulfide linkages with other thiol containing molecules, which could lead to protein aggregation. One would therefore expect thiol groups that do not participate in disulfide bonds crucial for proper folding and protein stability, to be buried inside the protein, which would provide a certain level of protection against undesirable modifications. It might however, also prevent any interaction of model proteins with silver nanoparticles immobilized on the surface of monoliths.

A literature search showed, that this indeed seems to be the case for most polypeptides that are commonly used as model proteins. Nevertheless, two proteins could be found, that do contain free thiol groups, which seem to be exposed to the outer surface to some degree.

The first one of these is human serum albumin. Crystallization studies reported that Cys34 in HSA is located in a loop on the protein surface. [19] Even though it may be protected to some degree

by the side chains of neighboring residues, it is still a much more likely candidate for interaction with silver nanoparticles than any cysteine residue buried deeply inside a protein.

Furthermore the Cys102 residue in cytochrome C from *Saccharomyces cerevisiae*, which is only partially buried in a hydrophobic pocket on the protein surface, has been reported to be accessible for immobilization on surfaces that have been derivatized with SH-terminated silanes. [20] As a result this molecule can also be expected to show retention on monolithic columns modified with silver nanoparticles.

Myoglobin, on the other hand doesn't contain any thiol groups at all. So it should be appropriate as a negative control sample.

3.3. *Synthesis of Silver nanoparticles*

DLS measurements suggested the presence of particles of two different sizes in the sample: smaller ones of approx. 8nm and larger ones of approx. 15nm.

The TEM pictures, however, show that there are particles of many different sizes present in the sample, ranging from approx. 2nm to maybe 15nm. All particles visible in the TEM pictures have a very regular spherical shape. This indicates that there are no aggregates present in the sample. (Figure 4, Figure 5)

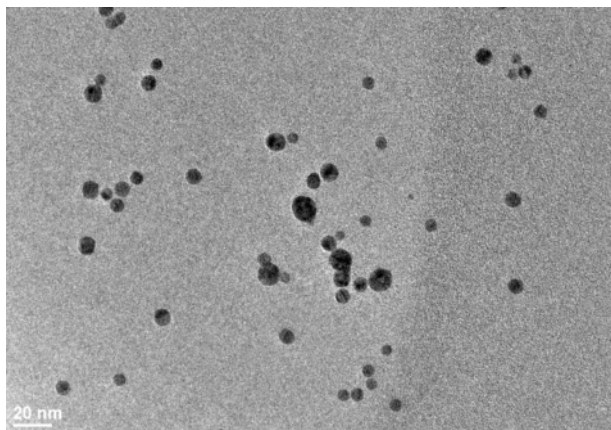


Figure 4 TEM: Bright Field, alpha 3, 200kV, 80k magnification

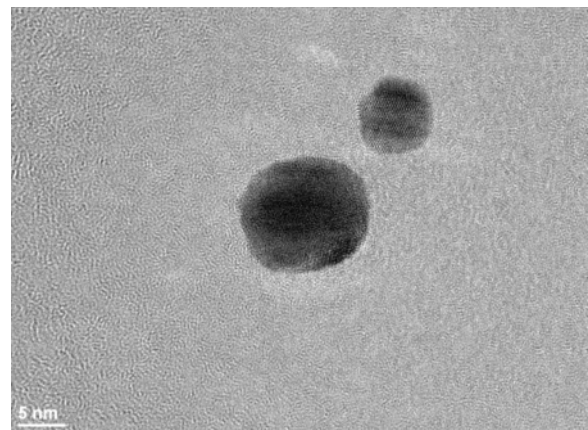


Figure 5 TEM: Bright Field, alpha 3, 200kV, 400k magnification

3.4. *Size distribution of Silver nanoparticles*

Size analysis of the Silver nanoparticle sample resulted in the following statistical values:

Mean	7.796304348 nm
SD	1.612192629
Min	4.58 nm
Max	12.81 nm
Data points	138

A histogram of the data shows a Gaussian-like distribution for the frequency of the various particles sizes with particles of sizes around 7nm being the most abundant.

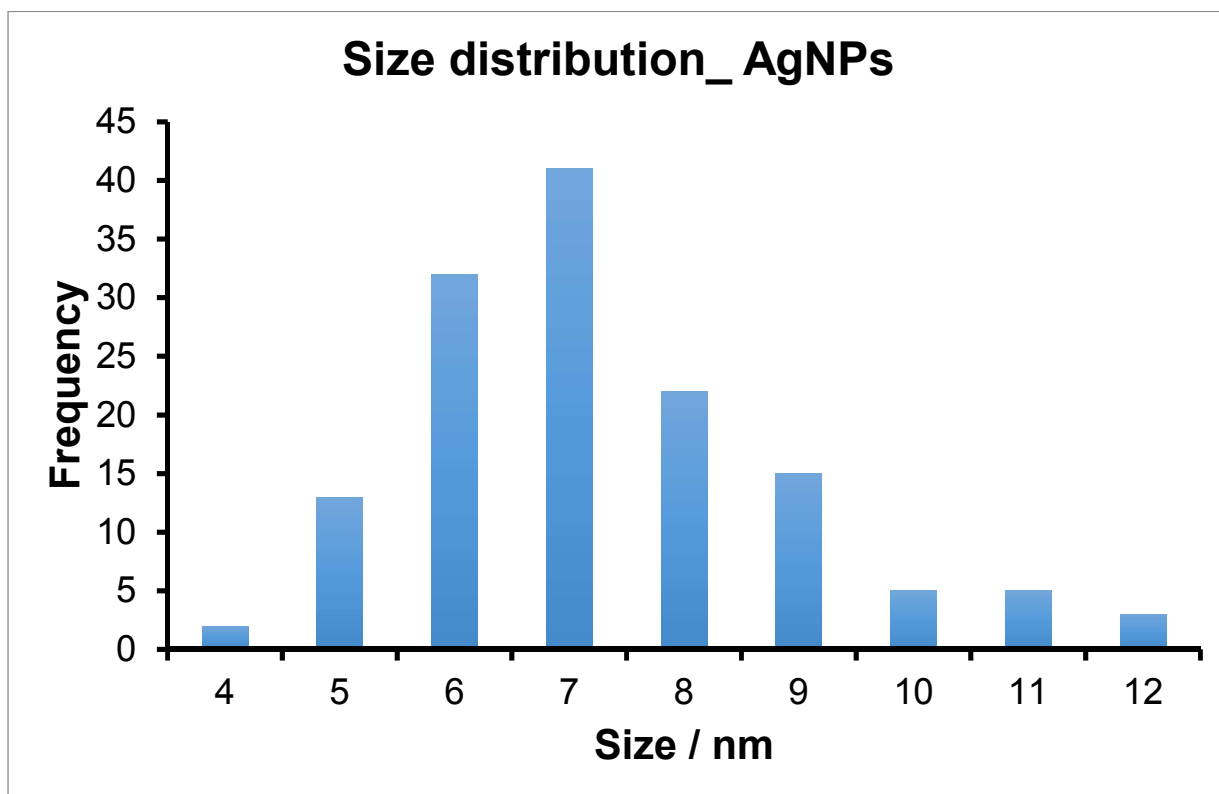


Figure 6 size distribution of silver nanoparticles

3.5. Column backpressure test

Backpressure tests were performed in order to determine the quality of the previously prepared monoliths. The acceptance criteria for further use of the columns was a backpressure of 5-8bar/cm column length. Table 1 shows the performance of the different monoliths and whether or not they were used for further modification steps for columns for batch 1, prepared in the first month, Table 2 shows the results for batch 2, prepared in the third month of the project.

Capillary #	Length [cm]	Pressure [bar]	p/L [bar/cm]	
1	16.7	93	5.6	✓
2	19.3	81	4.2	x
3	19.0	95	5.0	✓
4	19.1	92	4.8	?
5	18.1	98	5.4	✓
6	14.4	63	4.4	x
7	14.2	77	5.4	✓
8	14.9	67	4.4	x
9	14.7	50	3.4	x
10	14.7	66	4.5	x
11	14.7	91	6.1	✓
12	14.5	71	4.8	?
13	14.7	64	4.3	x

14	13.4	97	7.2	✓
15	14.8	95	6.4	✓
16	10.0	65	6.5	✓

Table 1 Backpressure test for column batch 1

Capillary #	Length [cm]	Pressure [bar]	p/L [bar/cm]	
17	24.3	190	7.8	✓
18	29.2	174	5.9	✓
19	23.8	185	7.8	✓
20	23.9	160	6.7	✓
21	24.1	160	6.6	✓
22	22.9	141	6.1	✓
23	24.6	133	5.4	✓
24	24.2	175	7.2	✓
25	24.3	130	5.3	✓
26	24.6	120	4.9	~
27	24.2	117	4.8	~

Table 2 Backpressure test for column batch 2

3.6. Modification with silver nanoparticles

For the first batch of columns the nanoparticle modification step seemed to be complete after approximately 2.5 hours, as a slightly yellow liquid was leaving the column, which suggests nanoparticles passing through. Those reaction times, however, were unusually short compared to what was previously experienced at the Lab for the modification of monoliths with gold nanoparticles.

For the second set of columns prepared later, the same modification step took approximately 24 hours. This discrepancy cannot be solely attributed to the increased column length (25 cm compared to 10 cm). Combined with later observed issue of nanoparticles being eluted from the column during chromatographic runs, it would rather indicate some sort of problem during the preparation of the first batch of columns, which resulted in unstable attachment of the nanoparticles on the monolithic surface for the first set of columns.

3.7. SEM pictures of silver nanoparticle coated monolith

Using scanning electron microscopy silver nanoparticles could be detected on the surface of the monolith. (Figure 7) This indicates successful surface modification of the through pores of the monolith.

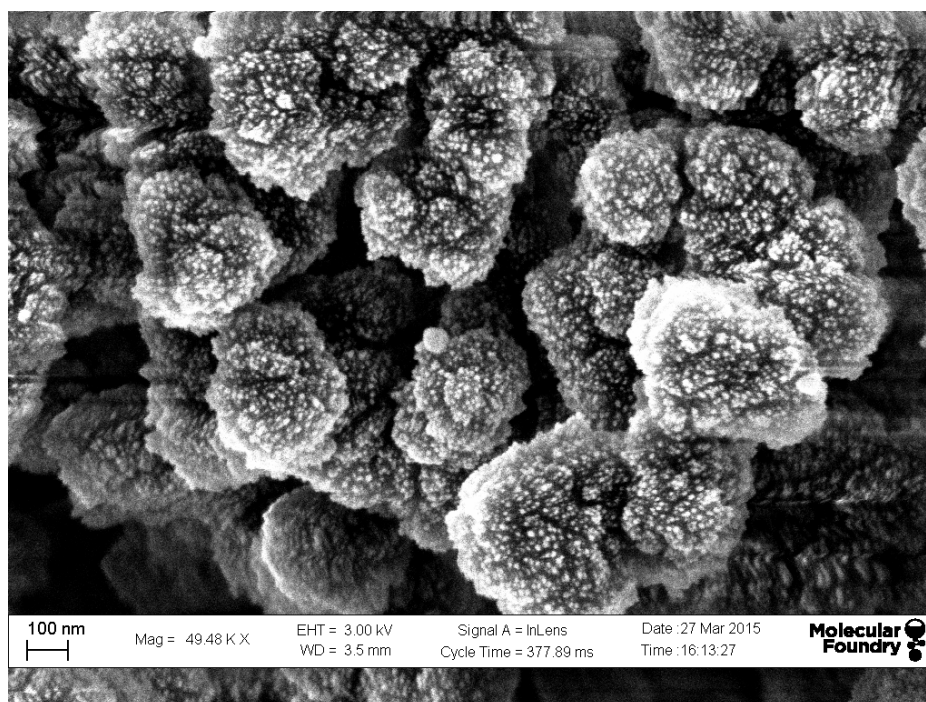


Figure 7 Monolith coated with silver nanoparticles

3.8. Testing of column dead volume

Acetone is a small molecule and should not be retained by the column. Injecting it into the HPLC system should therefore show how much time it takes for a molecule to pass through the column if there is no interaction with the stationary phase. This should give a reference point for future experiments to clearly identify retention due to interaction with the nanoparticles on the column.

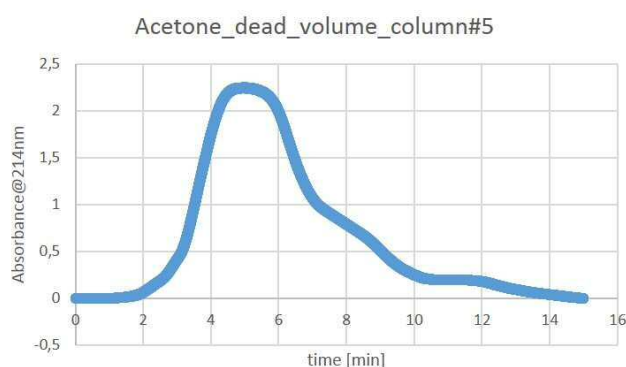


Figure 8 dead volume of column#5, measured with acetone

The peak visible in Figure 8 is comparatively broad and the experiment could probably be improved by using a smaller injection volume. 200 μ L is, however, the smallest volume possible with the loop currently mounted on the injection valve. Should it prove to be impossible to distinguish retained peaks from non-retained ones, the experiment could always be repeated using a smaller injection loop.

3.9. Retention of HSA on monoliths modified with silver nanoparticles

If free SH-groups in the model proteins bind to the silver nanoparticle on the monoliths, it should be possible to elute the proteins using other thiol containing compounds. In previous publications 2-mercaptoethanol has been used for that purpose. In order to avoid the intense smell of that substance 2-mercaptoethanesulfonate (MESNA) was tested as a thiol containing eluent instead. A solution containing 100mM MESNA in water was used as mobile phase B. Using the conditions described above, the chromatogram in Figure 9 could be obtained:

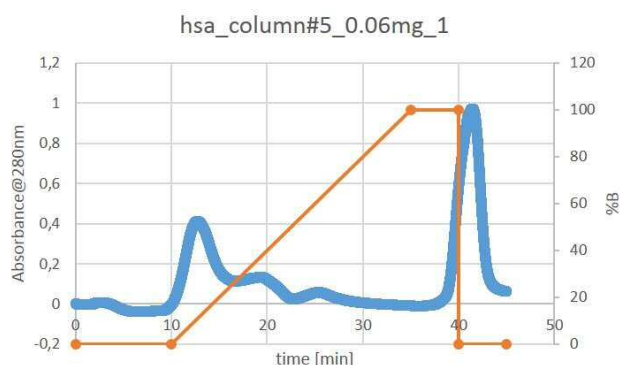


Figure 9 Retention of HSA monoliths modified with silver nanoparticles

The dead volume of the column was around 3 μ L, measured with acetone, so the peak at 10min is definitely the result of retention even though it may elute independently of the MESNA gradient, which had only just started at the elution time of this peak. It is not clear, however, if the second peak, eluting after approx. 40min is a protein peak or if the MESNA might be abolishing the binding of the nanoparticles to the surface of the monolith rather than eluting only the proteins from the column.

3.10. Regeneration of the nanoparticle column

After displacing proteins from the monolith by running a gradient of another thiol-containing molecule, there should no longer be sufficient numbers of interaction sites available for another cycle of protein binding. Therefore a regeneration procedure has to be established in order to remove the thiols introduced via the MESNA gradient from the column, preferably without affecting the nanoparticles immobilized on the monolithic surface. In theory, the binding of the nanoparticles to the monolith should be more stable than the interaction with the proteins, because there should be a much higher number of interaction sites available on the surface of the monolith, thereby fixing the nanoparticle in place by multiple interactions at once, whereas the protein-nanoparticle interaction is based on only a single free thiol on the protein surface. For gold-nanoparticle coated monoliths a regeneration procedure based on washing with water at elevated temperatures has been published. [15] Accordingly, regeneration was attempted by flushing the column with water at 65°C and 80°C for 2h each.

After regeneration at 65°C the chromatogram Figure 10 shows a peak eluting earlier than before at approx. 7min retention time. After 30min a broad elution front could be observed, that could

either be protein, that didn't elute from the column during previous runs, or nanoparticles coming of the column.

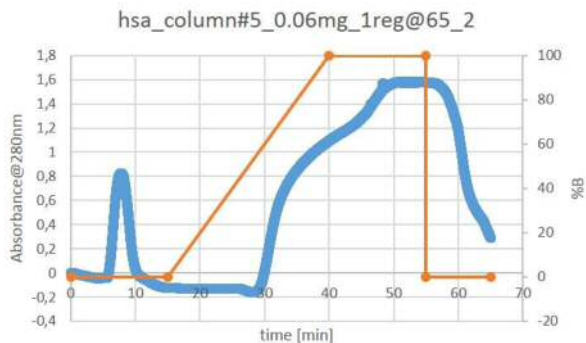


Figure 10 Injection of HSA after column regeneration at 65°C



Figure 11 injection of HSA after column regeneration at 80°C

A similar picture could be observed after regeneration at 80°C. (Figure 11) A peak was detected around 5min. After 25min a broad elution front was observed, that could either be protein or nanoparticles.

3.11. Detection of proteins and nanoparticles at different wavelengths

As previous experiments suggested that nanoparticles might be coming off the columns during the HPLC runs, a method to distinguish the soluble proteins from the disperse nanoparticles was needed. Theoretically any detector signal resulting from the nanoparticles would be based on light scattering rather than absorption and should therefore be visible at multiple wavelengths. The UV detection of proteins on the other hand is based on the absorption of aromatic amino acids present in the molecule, which is specific to 280nm. Except for certain proteins that form complexes with other prosthetic molecules, this class of biomolecules is not detectable at higher wavelengths. It should therefore be possible to distinguish signals coming from the proteins and the nanoparticles by using 2 different detection wavelengths, i.e. 280 and 350nm. A peak that is detectable at 280nm only would correspond to the protein, whereas any signal that shows up on both wavelengths simultaneously can't be attributed to the protein and should therefore correspond to nanoparticles leaving the column.

In order to test this hypothesis a series of experiments was performed. First nanoparticles were diluted in water and then injected into the HPLC system without using any column with signals detection at 280 and 350nm. Afterwards that experiment was repeated with a mixture of hsa (human serum albumin) and the diluted nanoparticles as well as with hsa alone.

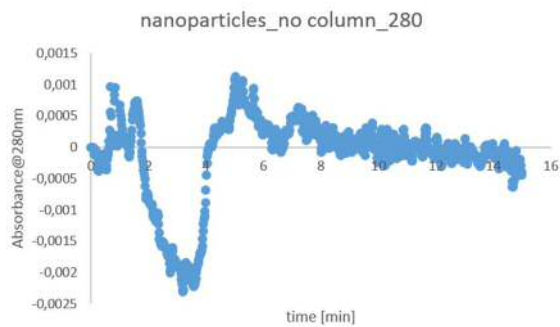


Figure 12 Injection of nanoparticles alone, detection at 280nm

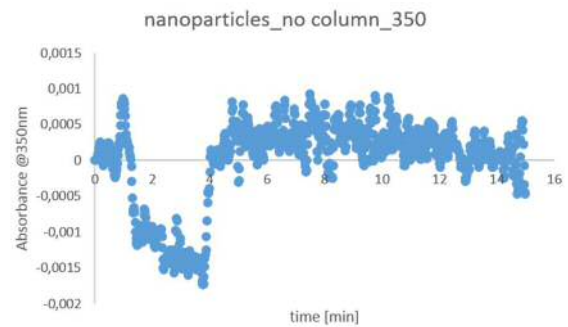


Figure 15 Injection of nanoparticles alone, detection at 350nm

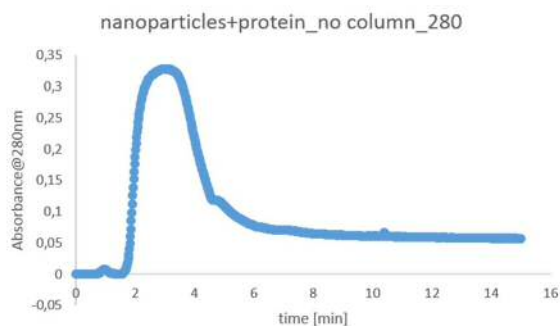


Figure 13 Injection of a mixture of nanoparticles and proteins, detection at 280nm

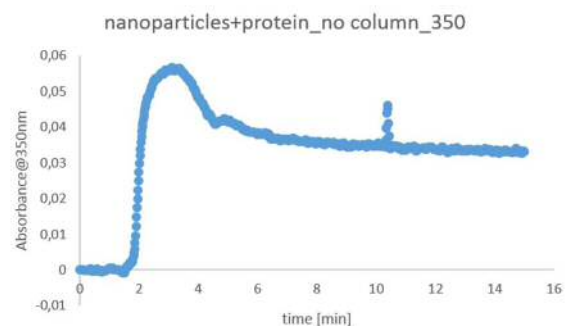


Figure 16 injection of a mixture of nanoparticles and protein, detection at 350nm

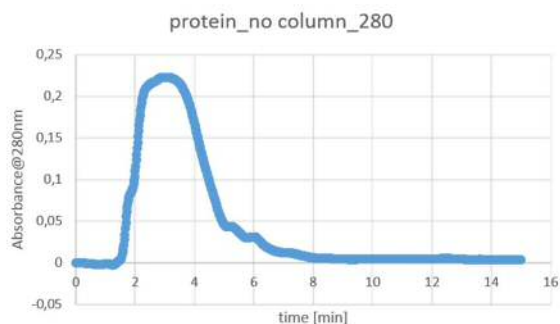


Figure 14 Injection of protein, detection at 280nm

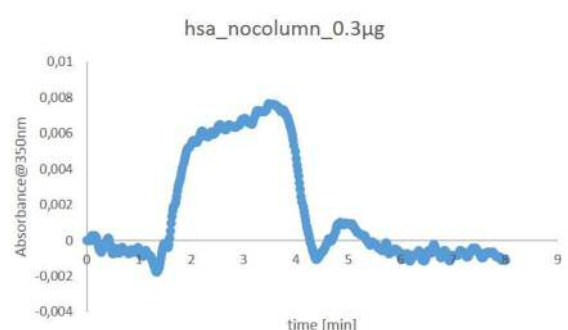


Figure 17 Injection of protein, detection at 350nm

Figure 12 – Figure 17 show the chromatograms obtained in these experiments. For the nanoparticles alone no proper signal could be obtained. Between 2 and 4 min into the experiments the signal drops below zero, however, the amplitude of this signal is so small, that it would not even be visible compared to any relevant peak like the ones obtained in Figure 13 and Figure 14. The mixture of nanoparticles and proteins on the other hand gives a clear signal at both wavelengths in the dead-volume range of the system. The peaks tail very strongly, especially at 350nm and don't drop back to the original baseline during the entire length of the run. As a result the HPLC was flushed with Acetonitrile for 2hours to get rid of any material that might be remaining in the system.

As expected the protein alone gave a good signal at 280nm (Figure 14). At the second detection wavelength a similar peak around 1.7 min could be observed. (Figure 17). The signal intensity, however, was much lower than for the protein-nanoparticle mixture. So it really seems to be possible to attribute strong signals observed at this wavelength to nanoparticles eluting from the column.

3.12. Elution of proteins with 3-mercaptopropionic acid

All attempts to use MESNA reagent for elution of proteins from the columns resulted in leeching of silver nanoparticles. It is possible that this is caused by an interaction of the sulfonate group of the MESNA reagent with the modified columns. In order to avoid that 3-mercaptopropionic acid was tried as an alternative eluent. Signals were detected at 280nm and 350nm.

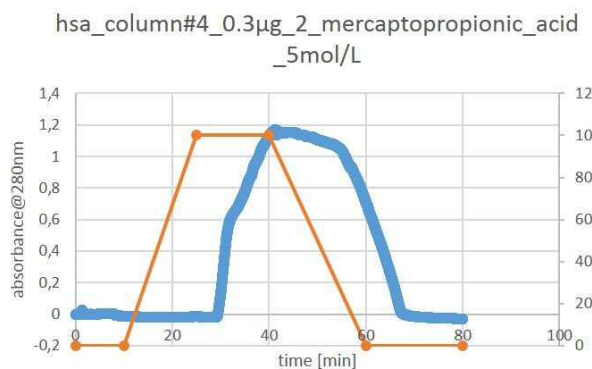


Figure 18 Retention of hsa on silver modified monolith, detection at 280nm

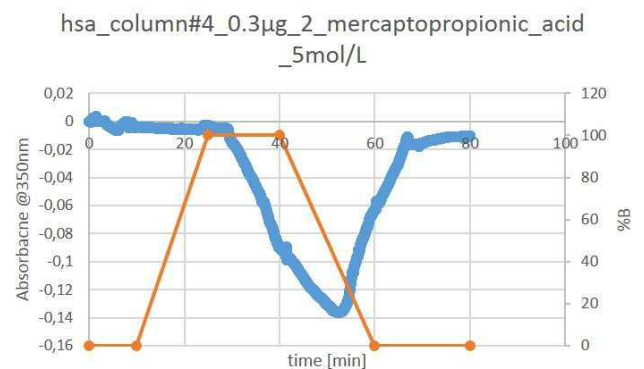


Figure 19 Retention of hsa on silver modified monolith, detection at 350nm

Injection of hsa (human serum albumin) on a silver modified monolith followed by a gradient of 5M 3-mercaptopropionic acid for elution resulted in a signal of very high intensity at 280nm. (Figure 18) This signal could not be caused by protein eluting from the column, as the same amount of protein had been injected in previous experiments resulting in a signal of much smaller peak area. That led to the idea that the signal increase might be caused by 3-mercaptopropionic acid itself. In order to test this hypothesis, water was injected into the HPLC system without any column connected to it, followed by the same gradient of 3-mercaptopropionic acid. In this experiment a similar 280nm signal could be observed. (Figure 20)

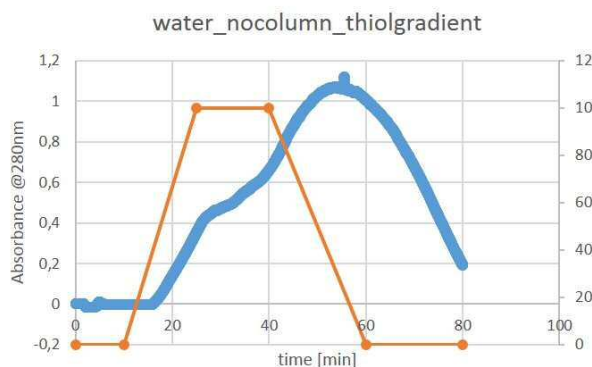


Figure 20 Injection of water, detection at 280nm

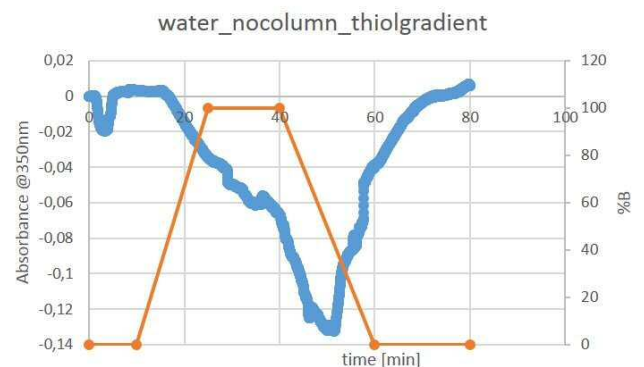


Figure 21 Injection of water, detection at 350nm

This 280nm signal of 2-mercaptopropionic acid is going to mask any protein that might be eluting from the column during the HPLC runs. It will therefore be necessary to either find an alternative eluent for further experiments or use an MS-detector connected to the HPLC in order to be able to distinguish proteins from 2-mercaptopropionic acid molecules eluting from the system.

3.13. Calculation of the amount of thiol groups needed to saturate the binding sites on a nanoparticle column

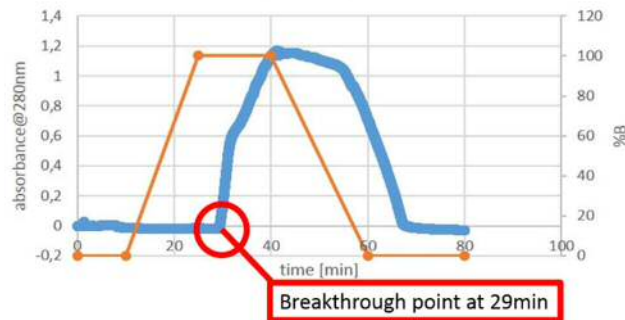


Figure 22 injection of hsa, attempted elution with 3-mercaptopropionic acid

Figure 22 shows the injection of hsa onto a newly prepared nanoparticle column followed by a gradient of 5mol/L 3-mercaptopropionic acid for elution. As explained above the signal that can be seen in the chromatogram is the result of the 280nm absorption of 3-mercaptopropionic acid rather than the elution peak of the protein. Theoretically it should be possible to estimate from this curve, how much of the thiol containing compound is necessary to saturate all the available binding sites of the column, which would be equivalent to the - protein capacity of the column for a protein that contains a single accessible thiol group. Furthermore this value would give an indication of the amount of thiol compound necessary to guarantee elution of proteins bound to the column, if this elution is possible.

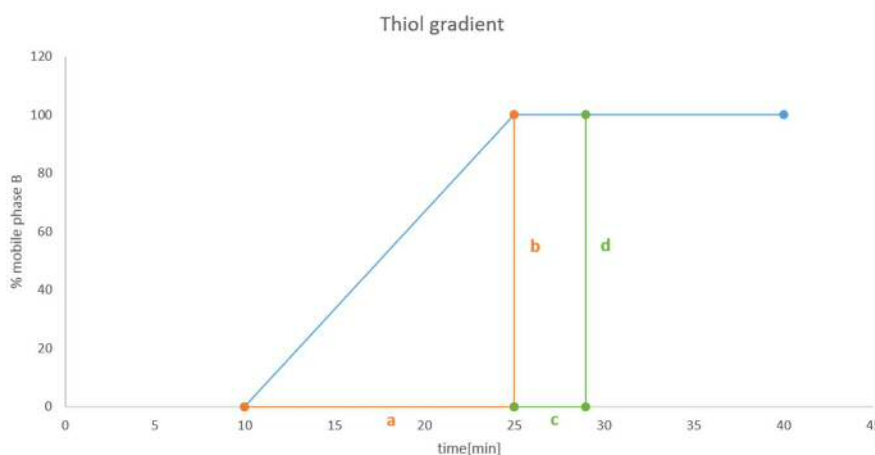


Figure 23 Thiol gradient used in HPLC experiments and calculation of thiols necessary for saturation of the column

Figure 22 shows the Thiol gradient used in the experiment described above in more detail. The area of the triangle formed with sites a and b should be equivalent to the amount of 3-

mercaptopropionic acid that passes through the system during the gradient. The rectangle formed by c and d corresponds to the phase after the gradient, when the column is flushed with mobile phase B only up to the break through point at 29 minutes that could be obtained from the chromatogram in Figure 22.

The area of the triangle can be calculated by the formula:

$$A_t = \frac{1}{2} \times a \times b = \frac{1}{2} 15min \times 100\% = 7.5min$$

The area of the rectangle can be calculated by the formula:

$$A_r = c \times d = 4min \times 100\% = 4min$$

Both combined would therefore correspond to 11.5 min of flushing with mobile phase B. At a flow rate of 1 μ L/min that corresponds to 11.5 μ L mobile phase B. Considering the concentration of 5mol/L this is equivalent to 57.5 μ mol 2-mercaptopropionic acid. As 3-mercaptopropionic acid contains 1 thiol group per molecule, this is the same as 57.5 μ mol thiols, which seem to be necessary to saturate all the available binding sites on the column and result in breakthrough for a monolith of approximately 23cm length.

Theoretically it would be necessary to subtract the system dead volume from the areas calculated above. This amount, however, is relatively small compared to the calculated volume of mobile phase B and should therefore not have too much impact on the calculation especially as the calculated value will only be used as an approximate reference point for further experiments.

In previous experiments a 100mmol solution of MESNA (Na 2-mercaptoethanesulfonate) has been used as mobile phase B for attempting protein elution. With this solution it would take almost 10 hours of flushing at 1 μ L/min to pump the necessary amount of 57.5 μ mol of thiols through this column. This indicates that the amount and concentration necessary to achieve any protein elution might simply be much higher than previously expected.

3.14. Elution attempt with longer MESNA gradient

A first attempt at calculating the amount of thiol groups needed for saturation of the columns resulted in a value of 6 μ L rather than 60 μ L due to a mistake in the calculation. As a result an experiment with a longer than usual MESNA gradient (15 min gradient from 0-100%B followed by 70 min flushing at 100% B) was conducted. The resulting chromatogram (Figure 24) shows a clear signal increase starting after approx. 80 min which continues until the end of the experiment. If this is indeed protein coming of the column, this would indicate, that indeed the amount of thiols used in previous experiments was much too small to achieve protein elution. However, that hypothesis would have to be tested in further experiments.

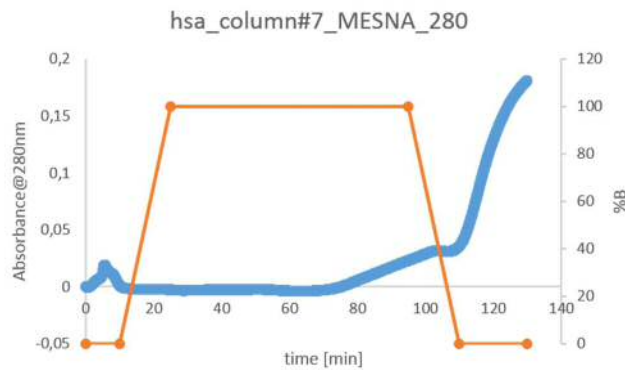


Figure 24 Attempted elution of hsa from nanoparticle column using a longer MESNA gradient

3.15. Unexpected Retention of Myoglobin

Myoglobin does not contain any SH-groups. It was therefore considered to be an appropriate negative control. Additionally myoglobin contains a Fe molecule as a prosthetic group in the active center. This protein-metal complex shows an absorption maximum around 410nm and could therefore be detected at that wavelength.

Injection of 200nL of a 1.5mg/mL solution of myoglobin, followed by an Acetonitrile gradient for washing of the column, however, resulted in no noticeable signal at a wavelength of 410nm. (Figure 25)

The same experiment was therefore repeated at a detection wavelength of 280nm. (Figure 26) Once again, no peaks were visible in the range of the dead volume of the system (around 2min). Peaks were detectable, however, during the Acetonitrile washing step. This would indicate that myoglobin too, is retained on the monolith, but can be eluted using an organic solvent. This retention, however, has to be based on some other mechanism than the interaction between thiol groups and silver, as there are no SH-groups present in myoglobin.

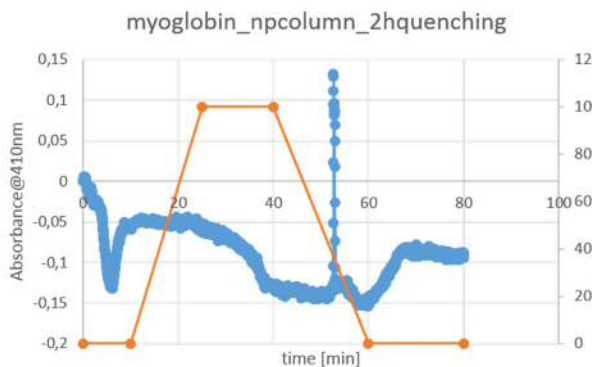


Figure 25 Myoglobin on nanoparticle column, detection at 410nm

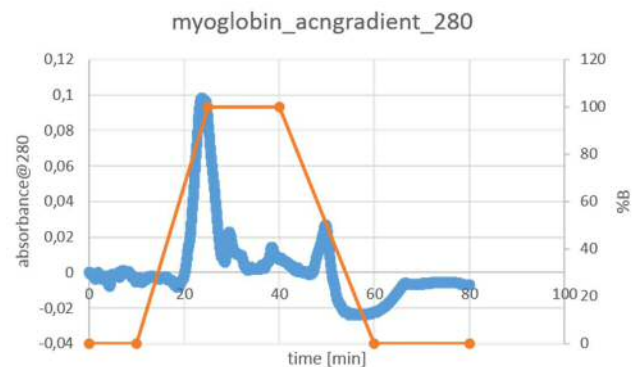


Figure 26 Myoglobin on nanoparticle column, detection at 280nm

The most obvious explanation for that seems to be that there could be other functional groups available on the column, remaining either from incomplete previous modification steps or from the hydrophobic material originally used to prepare the monolith. If any such functional groups

were indeed available on the nanoparticle columns, it seems logical that they should also be present on columns which had never been modified with nanoparticles, but had gone through all previous modification steps, including the TCEP-cleavage of immobilized cystamine. When myoglobin was injected onto one of these TCEP-column, however, a clear protein peak in the range of the dead volume was detectable at 280nm. (Figure 27) This indicates that the observed retention of myoglobin is mediated by the silver nanoparticles.

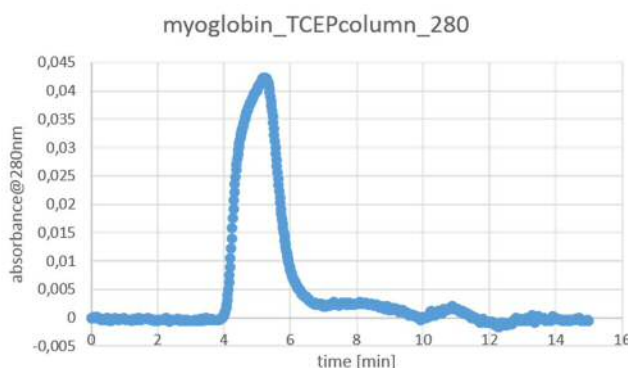


Figure 27 Myoglobin on TCEP-column, detection at 280nm

A literature search revealed, that adsorption of different heme proteins including myoglobin onto both gold as well as silver nanoparticles has been reported previously. [21, 22] Based on this, a retention of myoglobin on a silver nanoparticle modified monolith based on non-specific affinity of the protein towards the silver nanoparticles does seem to be a possible explanation for the observed retention.

3.16. HPLC-MS experiments:

Due to the 280nm absorption that 3-mercaptopropionic acid showed in previous experiments, it was not possible to use an ordinary UV-detector at the protein wavelength of 280nm for detection. A more suitable alternative would be an HPLC instrument connected to a mass spectrometer as a detector, which is also available at the Berkeley lab. In order to check the performance of the instrument, first of all myoglobin was injected via the HPLC injector using water as a mobile phase and the resulting MS signal was recorded by the instrument. (Figure 28) The series of peaks between m/z ratios of 800-1500 show the typical profile that is to be expected for proteins in mass spectrometry. Signal deconvolution and calculation of the actual compound mass corresponding to those signals results in a value of 16967.7 Da. The theoretical mass of myoglobin listed in the literature is 16952.56 Da, which corresponds reasonably well with the observed signal, given that the instrument was not calibrated right before the experiment. However, there is also a background signal of rather large intensity visible in the lower m/z range of the spectrum, which indicates a contamination somewhere in the system. This problem became even more pronounced, when the experiment was repeated using acetonitrile as a mobile phase instead of water. Here the background signal shifted to even higher m/z ratios (Figure 29). The signal that could finally be obtained, when injecting myoglobin dissolved in water, but with acetonitrile as a mobile phase, looked like a combination of the

protein signal in water and the background signal in acetonitrile. (Figure 30) This suggests, that there is indeed a contamination present somewhere in the system, either in the HPLC- or in the MS-part of the instrument and that part of it gets washed out when organic solvent is used.

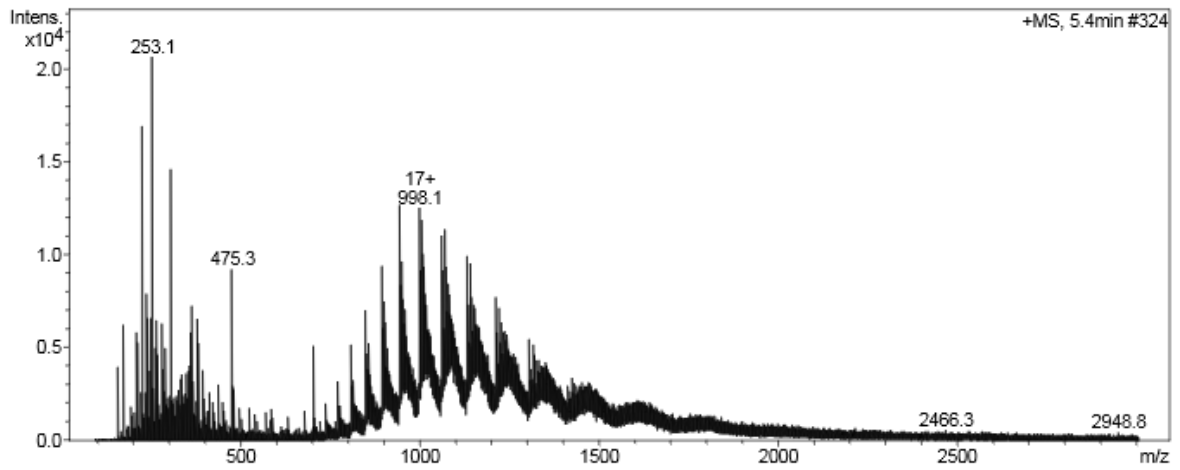


Figure 28 MS-spectrum for myoglobin, water as mobile phase

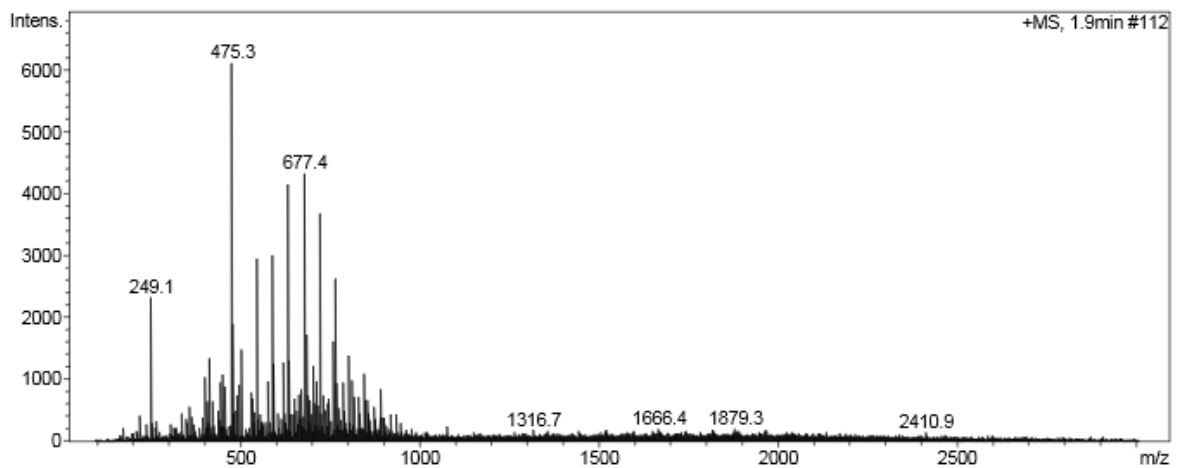


Figure 29 background signal in acetonitrile

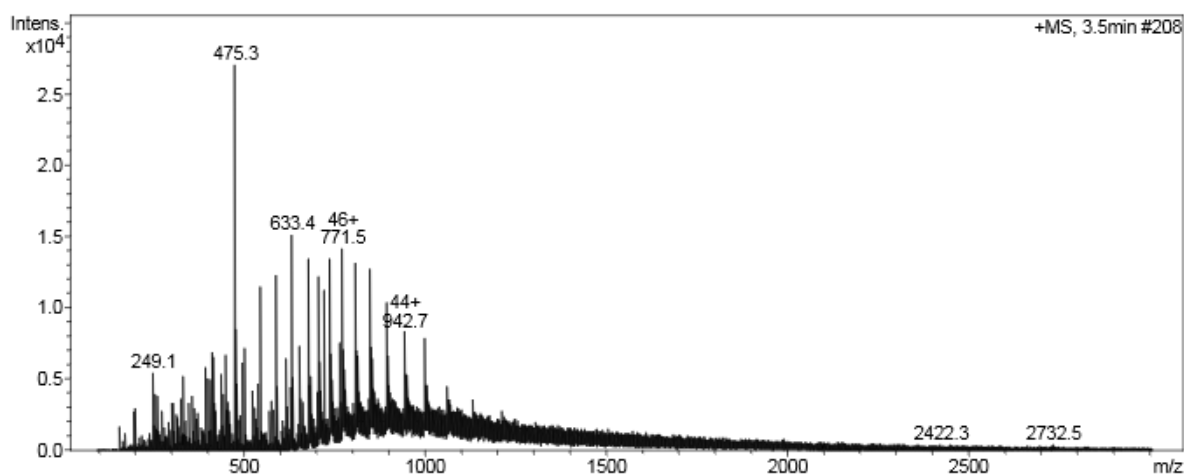


Figure 30 MS-spectrum for myoglobin, acetonitrile as mobile phase

In the interest of time, it seemed to be the best course of action to stop HPLC experiments at this point and use the remaining time in Berkeley for preparing columns instead, which could be brought back to Vienna, where an HPLC-MS system in better shape is available for further use. In the remaining three weeks 20 new nanoparticle monoliths were prepared, as well as 5 additional cystamine-modified ones and 3 TCEP-cleaved columns.

4. Conclusion

Most of the goals stated in the research proposal for this work could be met during the time at the Berkeley Laboratory. Laboratory-made silver nanoparticles of appropriate sizes could be obtained via chemical synthesis and characterized using a Transmission Electron Microscope (TEM). Stable and fully functional monolithic columns could be created. Furthermore, surface modification of these monoliths with the self-made silver nanoparticles was possible following the proposed modification scheme. Presence of nanoparticles on the surface of the pores of the monoliths was demonstrated beyond doubt using Scanning Electron Microscopy (SEM).

Additionally, it was shown in a series of chromatographic experiments, that the custom-modified silver nanoparticle monoliths are indeed able to retain proteins that have accessible free SH-groups on the surface

Due to unexpected problems with both, the instrumental equipment and the intended elution media, it was, however, not possible to determine whether it might be feasible to develop an actual separation methodology on this observed retention behavior. Thiol containing reagents like 3-mercaptopropionic acid seem to absorb at 280nm, which is also the detection wavelength normally used for proteins. As a result any possible elution peak caused by the protein sample leaving the column will always be masked by the much larger signal increase caused by mobile phase B and will therefore not be recognizable in the chromatogram.

Due to a lack of time and the instrumental problems with the HPLC-MS system at the Berkeley Laboratory, it was not possible to tackle that question in Berkeley. Instead, 20 new silver nanoparticle modified monolithic columns were prepared during the last weeks of August and then shipped to Vienna. These columns will now be used to carry out the remaining experimental work here at Boku, where multiple working HPLC-MS systems are available.

5. References

1. Aggarwal, S., *What's fueling the biotech engine* 2012 to 2013. *Nat Biotech*, 2014. **32**(1): p. 32-39.
2. Liu, H., et al., *Heterogeneity of monoclonal antibodies*. *J Pharm Sci*, 2008. **97**(7): p. 2426-47.
3. van Beers, M.M. and M. Bardor, *Minimizing immunogenicity of biopharmaceuticals by controlling critical quality attributes of proteins*. *Biotechnol J*, 2012. **7**(12): p. 1473-84.
4. Lingg, N., et al., *Highly linear pH gradients for analyzing monoclonal antibody charge heterogeneity in the alkaline range*. *J Chromatogr A*, 2013. **1319**: p. 65-71.
5. Lingg, N., et al., *Highly linear pH gradients for analyzing monoclonal antibody charge heterogeneity in the alkaline range: Validation of the method parameters*. *J Chromatogr A*, 2014. **1373**: p. 124-30.
6. Hjertén, S., J.-L. Liao, and R. Zhang, *High-performance liquid chromatography on continuous polymer beds*. *Journal of Chromatography A*, 1989. **473**: p. 273–275.
7. Minakuchi, H., et al., *Octadecylsilylated porous silica rods as separation media for reversed-phase liquid chromatography*. *Anal Chem*, 1996. **68**(19): p. 3498-501.
8. Svec, F. and J.M. Fréchet, *New designs of macroporous polymers and supports: from separation to biocatalysis*. *Science*, 1996. **273**(5272): p. 205-11.
9. Svec, F. and C.G. Huber, *Monolithic materials: Promises, challenges, achievements*. *Anal Chem*, 2006. **78**(7): p. 2101-7.
10. Barroso, T., et al., *Functional monolithic platforms: chromatographic tools for antibody purification*. *Biotechnol J*, 2013. **8**(6): p. 671-81.
11. Vlach, E.G. and T.B. Tennikova, *Preparation of methacrylate monoliths*. *J Sep Sci*, 2007. **30**(17): p. 2801-13.
12. Li, Y. and M.L. Lee, *Biocompatible polymeric monoliths for protein and peptide separations*. *J Sep Sci*, 2009. **32**(20): p. 3369-78.
13. Lv, Y., et al., *Preparation of porous polymer monoliths featuring enhanced surface coverage with gold nanoparticles*. *J Chromatogr A*, 2012. **1261**: p. 121-8.
14. Hilder, E.F., F. Svec, and J.M. Fréchet, *Latex-functionalized monolithic columns for the separation of carbohydrates by micro anion-exchange chromatography*. *J Chromatogr A*, 2004. **1053**(1-2): p. 101-6.
15. Xu, Y., et al., *Porous polymer monolithic column with surface-bound gold nanoparticles for the capture and separation of cysteine-containing peptides*. *Anal Chem*, 2010. **82**(8): p. 3352-8.
16. Krenkova, J., F. Foret, and F. Svec, *Less common applications of monoliths: V. Monolithic scaffolds modified with nanostructures for chromatographic separations and tissue engineering*. *J Sep Sci*, 2012. **35**(10-11): p. 1266-83.
17. Sapsford, K.E., et al., *Functionalizing nanoparticles with biological molecules: developing chemistries that facilitate nanotechnology*. *Chem Rev*, 2013. **113**(3): p. 1904-2074.
18. Sedlacek, O., et al., *Silver-coated monolithic columns for separation in radiopharmaceutical applications*. *J Sep Sci*, 2014. **37**(7): p. 798-802.
19. Sugio, S., et al., *Crystal structure of human serum albumin at 2.5 Å resolution*. *Protein Eng*, 1999. **12**(6): p. 439-46.

20. Gerunda, M., et al., *Grabbing yeast iso-1-cytochrome c by Cys102: an effective approach for the assembly of functionally active metalloprotein carpets*. Langmuir, 2004. **20**(20): p. 8812-6.
21. Tom, R.T., et al., *Hemoprotein bioconjugates of gold and silver nanoparticles and gold nanorods: structure-function correlations*. Langmuir, 2007. **23**(3): p. 1320-5.
22. Tom, R.T. and T. Pradeep, *Interaction of azide ion with hemin and cytochrome c immobilized on Au and Ag nanoparticles*. Langmuir, 2005. **21**(25): p. 11896-902.